Uptake of long-chain fatty acids in HepG2 cells involves caveolae: analysis of a novel pathway

Jürgen Pohl,[1] Axel Ring,[1] and Wolfgang Stremmel[2]

Department of Internal Medicine IV, Ruprechts-Karls-University, Heidelberg, Germany

Abstract   We investigated the role of caveolae in uptake and intracellular trafficking of long chain fatty acids (LCFA) in HepG2 human hepatoma cells. The uptake of [^{3}H]oleic acid and [^{3}H]stearic acid into HepG2 cells was measured by radioactive assays and internalization of the non-metabolizable fluorescent fatty acid 12-(N-methyl)-N-[(7-nitrobenz-2-oxa-1,3-diazol-4-yl)amino] (12-NBD) stearate into single HepG2 cells was semi-quantitatively assessed by laser scanning microscopy. The initial rate of [^{3}H]oleic acid uptake (V$_0$) in HepG2 cells exhibited saturable transport kinetics with increasing concentrations of free oleic acid (V$_{max}$ 854 ± 46 pmol mg protein^{-1} min^{-1}, K$_m$ 100 ± 14 nmol/l). While inhibition of clathrin coated pits did not influence LCFA uptake in HepG2, inhibition of caveolae formation by filipin III, cyclodextrin, and caveolin-1 antisense oligonucleotides resulted in reduction of [^{3}H]oleic acid uptake by 54%, 45%, and 23%, respectively. Furthermore, filipin III inhibited the uptake of [^{3}H]stearic acid and its fluorescent derivative 12-NBD stearate by 44% and 50%, respectively. Transfection studies with α-caveolin-1/cyanofluorescent protein chimeras showed significant colocalization of caveolae and internalized 12-NBD stearate.🔬 In conclusion, these data suggest a significant role for caveolae mediated uptake and intracellular trafficking of LCFA in HepG2 cells.—Pohl, J., A. Ring, and W. Stremmel. **Uptake of long-chain fatty acids in HepG2 cells involves caveolae: analysis of a novel pathway.** *J. Lipid Res.* 2002. **43**: 1390–1399.

Supplementary key words   vesicles • hepatocytes • intracellular trafficking • oleic acid

Long-chain fatty acids (LCFAs) serve a number of important biological functions as energy substrates (1), as precursors for glyco- and phospholipid components of cell membranes (2), as biological mediators like eicosanoids (3), and as mediators of cellular processes (e.g., gene expression and growth regulation) (1, 2). These multiple roles suggest that careful regulation of cellular uptake and utilization of LCFA is essential to cellular homeostasis.

However, the general issue of cellular LCFA uptake was controversial until today. Passage of LCFA across cell membranes has traditionally been considered to occur by passive diffusion through the membrane bilayer, with the transmembrane gradient being the driving force for the direction of net movement. Studies in model membrane systems (4–6) have shown that the protonized LCFA species can cross a protein-free phospholipid bilayer rapidly by a flip-flop mechanism. The diffusion hypothesis is challenged by the identification of a number of membrane-associated fatty acid binding proteins (7–11) that might be involved in facilitated fatty acid uptake: fatty acid translocase (FAT/CD36), the fatty acid transport protein (FATP) family, plasma membrane fatty acid binding protein (FAB-P$_{pm}$), and caveolin-1. The latter is the 22 kDa major structural protein of caveolae. Since caveolin-1 was shown to have a fatty acid binding site that binds fatty acids saturably with high affinity (10), we investigated involvement of caveolin-1 and caveolae in LCFA uptake and transport in HepG2 cells.

Caveolae are 50–100 nm flask-shaped invaginations of the plasma membrane that are biochemically characterized by their enrichment in cholesterol, glycolipids, and caveolin. They participate in several crucial cellular functions such as signal transduction (12), regulation of glucose uptake (13), cholesterol transport (14), potocytosis (15), and fluid-phase and receptor-mediated endocytosis (16, 17). Several studies have provided evidence for the internalization and trafficking of different ligands through caveolae to specific target sites, e.g., endosomes (18), or the Golgi apparatus (19). Recently, it was reported that in the hepatocyte, caveolae are mainly localized to the sinusoidal blood-facing plasma membrane (20, 21) represent-

Abbreviations: CFP, cyano-fluorescent protein; FAT, fatty acid translocase; FABP, fatty acid binding protein; FATP, fatty acid transport protein; LCFA, long-chain fatty acids; LSM, laser scanning microscopy; 12-NBD, 12-(N-methyl)-N-[(7-nitrobenz-2-oxa-1,3-diazol-4-yl)amino].

[1] J.P. and A.R. contributed equally to this work.
[2] To whom correspondence should be addressed.
   e-mail: wolfgang.stremmel@med.uni-heidelberg.de

ing dynamic structures that cycle between the cell surface and the endocytic compartment (20). Research on the role of caveolae in transport processes has been significantly facilitated by the finding that this pathway can be selectively inhibited by cholesterol depletion (16) and by modulation of caveolin-1 expression (22, 23). The potential involvement of caveolae in LCFA transport has not been focused on in previous studies. Our experiments based both on biochemical and molecular caveolae inhibition studies as well as the microscopic visualization of LCFA transport suggest that in HepG2 cells, caveolae may be operative in LCFA uptake and intracellular trafficking. We used HepG2 cells in our study, as this cell line has been shown to be a good model system to study fatty acid uptake and metabolism (24, 25).

MATERIALS AND METHODS

Materials

12-(*N*-methyl)-*N*-[(7-nitrobenz-2-oxa-1,3-diazol-4-yl)amino]octadecanoic acid (12-NBD stearate) and Mito-Tracker Red CMX Ros were obtained from Molecular Probes (Eugene, Oregon). [³H]oleic acid (60 Ci/mmol; 1 Ci = 37 GBq) and [³H]stearic acid were from Biotrend (Cologne, Germany). Human ¹²⁵I-labeled transferrin was purchased from NEN (Boston, MA), D-[2-³H]glucose was from Amersham (Little Chalfont, England). Fatty acid-free BSA (fraction V), cyclodextrin, ouabain, filipin III, sodium azide, 2,4-dinitrophenol, coenzyme A (CoA), and non-radioactive oleic acid and stearate were purchased from Sigma Chemical (St. Louis, Missouri). Lipofectamine plus reagent were purchased from Gibco (Paisley, Scotland). Ultima Gold scintillation fluid was from Packard (Groningen, Netherlands). The murine monoclonal antibody against caveolin-1 was from Transduction Laboratories (Lexington, Kentucky). The secondary antibody was obtained from Sigma Chemical. Western Blots were detected using the ECL reagents (Amersham).

Cell culture

HepG2 cells were grown to confluence in RPMI medium (Bio Whittaker, Walkersville) supplemented with 5% fetal calf serum.

Assay of fatty acid uptake

The [³H]oleic acid uptake assays were performed as described previously (26) using confluent HepG2 cell monolayers. Briefly, trace amounts of [³H]oleic acid mixed with measured quantities of nonradioactive oleic acid were dissolved in a defatted BSA solution (173 μmol/l) at different ratios varying from 0.1 to 2.0. Three milliliters of the oleate-BSA solution were incubated with each Hep G2 cell monolayer in a 5 cm Ø culture dish at 37°C. The uptake was stopped by removal of the solution followed by addition of 5 ml of an ice-cold stop solution containing 0.5% (wt/v) albumin. The stop solution was discharged after 2 min, and the culture dishes were washed by dipping them six times in ice-cold incubation buffer. NaOH (2 mol/l) was added to lyse the cells, and aliquots of the lysate were used for protein and radioactivity determination. Radioactivity was determined after the addition of 10 ml Ultima-Gold (Packard, Groningen, The Netherlands) in a 1,217 Rackbeta liquid scintillation counter (LKB-Wallac, Turku, Finland). The concentrations of unbound fatty acids in [³H]oleic acid/albumin solutions (fixed BSA concentration = 173 μmol/l, oleic acid:BSA molar ratios ranging from 0.1 to 2) were calculated by the stepwise equilibrium constant of

Wosilait and Nagy (27), using the dissociation constants for the oleic acid/albumin complex reported by Spector et al. (28).

Assays of ¹²⁵I-transferrin uptake

Incubation with ¹²⁵I-transferrin was performed as described by Lamb et al. (29) for one, five, or 10 min using filipin III-treated versus control monolayers of Hep G2 cells.

Separation of cellular lipids by TLC

The incorporation of [³H]oleic acid into cellular lipids was determined after incubation of 173 μmol/l [³H]oleic acid-albumin (1:1, mol/mol) with confluent HepG2 monolayers as described above. Cell lysates were extracted three times in 4 ml of chloroform-methanol (2:1, vol/vol). The extracts were pooled and 0.2 vol of water were added to separate out an aqueous phase. The chloroform phase was evaporated under a stream of nitrogen, then redissolved in 200 μl of chloroform-methanol (2:1, vol/vol), and applied to silica gel plates (DC-Fertigplatte Kieselgel 60 F₂₅₄, Merck, Darmstadt, F.R.G.). The developing solvent was hexan-diethyl ether-acetic acid (25:4:0.3, v/v/v). Lipids were stained by I₂ vapor. After sublimation of I₂, each spot was scraped directly into a scintillation vial for measurement of radioactivity.

Semiquantitative measurement of 12-NBD stearate uptake using laser scanning microscopy

This method using an upright Zeiss laser scanning microscopy (LSM) 310 system (Zeiss, Oberkochen, Germany) has been previously described by us in detail (30). Briefly, uptake studies were performed in HEPES-buffered saline containing 135 mmol/l NaCl, 5 mmol/l KCl, 0.8 mmol/l MgSO₄, 0.12 mmol/l CaCl₂, 0.8 mmol/l Na₂HPO₄, 10 mmol/l HEPES (pH 7.4), and 5 mmol/l glucose. Both the albumin and stearate concentrations were 173 μmol/l. Of the stearate component, 23 μmol/l were 12-NBD stearate and 150 μmol/l non-fluorescent stearate.

Culture dishes were preincubated for 30 min at 37°C in HEPES-buffered saline containing filipin III (5 μg/ml). Controls received HEPES-buffered saline without filipin III. Following preincubation, the slides were placed on the stage of the microscope and superfused with HEPES-buffered saline containing 12-NBD stearate at a rate of 40 ml/min. Individual HepG2 cells were identified with a ×40 Plan-Neofluar multi-immersion objective (numerical aperture 0.9) (Zeiss, Oberkochen, Germany) by conventional light microscopy. The system was then switched to the frame mode and a confocal picture was generated with the 488 nm line of the argon laser (attenuation = 10) for uptake studies with 12-NBD stearate. The emission light was recorded by a photo multiplier after passing a 525 nm to 565 nm band-pass filter under manual gain and black level control. The increase in intracellular fluorescence afforded by cellular 12-NBD stearate uptake was recorded as arbitrary units, with zero units being the background fluorescence of HEPES-buffered saline. The fluorescence intensity in a "region of interest" within the cytosol was plotted against the time in order to obtain a semi-quantitative determination of 12-NBD stearate uptake.

Effects of antisense oligonucleotides

Phosphorothioate-substituted antisense oligonucleotides to human caveolin-1 (5′-CAG TGA AGG TGG TGA AG) and antisense oligonucleotides to human clathrin (5′-CTG GGT CAG CCT GT) have been designed and manufactured by Biognostik (Göttingen, Germany). The equivalent sense strands served as controls. Transfection of oligonucleotides was performed using lipofection reagent and 2 μg of DNA per 35 mm dish according to the manufacturer's manual. Efficiency of intracellular uptake of antisense strands into HepG2 cells was monitored by fluorescence labeled caveolin-1 and clathrin oligonucleotides in control

experiments. Treatment of HepG2 cells with antisense oligonucleotides was carried out for 3 days at 37°C. Subsequently, the reduction of caveolin-1 or clathrin protein levels by antisense treatment was assessed by separating 50 µg of total cell protein on an SDS gel and subsequent Western blotting as described below.

Western blot analysis

HepG2 cells were lysed in 50 mmol/l Tris-HCl (pH 7.4) containing 1% TritonX 100, 150 mmol/l EDTA, and antiproteases (1 mmol/l PMSF, 1 µg/ml pepstatin, and 1 µg/ml leupeptin). The protein concentration was quantified by the Bradford procedure (BioRad). Fifty micrograms of total cell protein were separated by 12% SDS-PAGE and transferred to nitrocellulose membranes. Ponceau-S staining was used to confirm even transfer. Caveolin-1 and clathrin-heavy chain were detected using a murine monoclonal antibody at a dilution of 1:2,000 and a peroxidase-coupled secondary anti-mouse antibody (all from Transduction Laboratories, Lexington, Kentucky). Antibody binding was visualized using the ECL reagents (Amersham).

Construction and transfection of α-caveolin-1/cyano-fluorescent protein fusion protein

α-Caveolin-1/green fluorescent protein (GFP) was kindly provided by Dr. Hiroshi Kogo (Nagoya University School of Medicine, Japan). Caveolin-1 DNA was excised from this construct and fused in-frame C-terminally to cyano-fluorescent protein (CFP) using the pECFP-C1 vector (Clontech, Inc.). Transfection of the plasmid construct was performed using lipofection reagent and 2 µg of DNA per 35 mm dish as instructed by the manufacturer's manual. After transfection, HepG2 cells were either fixed and stained with anti-caveolin-1 antibody, or incubated with 12-NBD stearate (23 µmol/l) plus non-fluorescent stearate (150 µmol/l) solubilized by albumin (173 µmol/l) for 2 min. Cells were directly visualized with an inverted Olympus IX50 system with a ×100 u-plan apo objective (numerical aperature 1.35) using a cyan (D436/20; D480/44; Olympus, Hamburg, Germany) and green fluorescent filter system (BP450-480/BA515; Olympus).

Immunocytochemistry

HepG2 cells that expressed α-caveolin-1/CFP fusion protein were washed three times in PBS and fixed in 2% paraformaldehyde. The first antibody was applied for 4 h at a dilution of 1:500 (v,v) at 4°C followed by washing three times with 0.05 mmol/l Tris-HCl, pH 7.4. The second antibody was applied for 2 h at 4°C diluted 1:500 (v,v) in 0.05 mmol/l Tris-HCl, pH 7.4.tetramethyl cholamine isothiocyanate (TRITC)-labeled second antibody was detected by a TRITC filter system (UMNG; BP530–550/BA590; Olympus).

Statistical analysis

Results are given as means ± SD. Student's *t*-test was used to test for significant difference among means. Linear and non-linear regression models were used to analyze the effect of free oleic acid concentration on the rate of initial uptake and to determine the mathematical model that best described the experimental data.

RESULTS

Uptake as a function of the external fatty acid concentration

To confirm that HepG2 cells adequately reflect the known properties of primary hepatocytes with regard to LCFA influx, we examined uptake of [³H]oleic acid at var-

ious concentrations of free oleic acid in the incubation medium (**Fig. 1**). The unbound oleic acid concentration was modulated without exceeding its solubility by incubation of a fixed concentration of albumin (173 µmol/l) and increasing concentrations of [³H]oleic acid. The initial rate of uptake was determined by linear regression fit from uptake measured over the initial 20 s incubation period. The best-fit parameters are $V_{max} = 854 \pm 46$ pmol mg protein^{-1} min^{-1} and $K_m = 100 \pm 14$ nmol/l, which is comparable to the kinetics of initial [³H]oleic acid uptake by primary hepatocytes (26).

## Effect of metabolic inhibitors on [³H]oleic acid uptake

To further validate the HepG2 cell model for LCFA uptake, cells were treated with different transport and metabolic inhibitors known to influence LCFA transport in primary hepatocytes. After a 30 min pretreatment, HepG2 cells were incubated with equimolar ratios of albumin and [³H]oleic acid (173 µmol/l) for 5 min. Pretreatment with sodium azide (50 mmol/l) or antimycin A (25 µmol/l) reduced [³H]oleic acid uptake to $19 \pm 2\%$ and $27 \pm 6\%$ of control levels. Likewise, ouabain (0.5 mmol/l), an inhibitor of the Na$^+$/K$^+$-ATPase in rat hepatocytes, and phloretin (0.4 µmol/l), a potent inhibitor of cellular transport processes, reduced the uptake of [³H]oleic acid to $61 \pm 13\%$ and $30 \pm 9\%$ of control levels, respectively (data not shown). This inhibition pattern is consistent with previously reported characteristics of LCFA uptake by human hepatocytes (7, 26). Taken together, these results confirm that HepG2 cells adequately reflect the known properties of primary hepatocytes with regard to LCFA uptake.

Effect of filipin III on [³H]oleic acid uptake

Cholesterol is a crucial component required to maintain the structural integrity of caveolae. Exposure of cells to filipin III, a sterol-binding agent, preferentially removes cholesterol from the plasma membrane, causing disappearance of caveolae (16, 31). We investigated the effects of filipin III treatment on LCFA uptake in HepG2 cells. After 30 min of preincubation with filipin III (5 µg/ml, 37°C), [³H]oleic acid accumulation was significantly reduced (**Fig. 2**). This inhibitory effect was increasing over time, suggesting that filipin III interferes predominantly with a late uptake phase. While in control cells the time dependence of [³H]oleic acid uptake was almost linear, filipin III treatment resulted in a non-linear relationship characterized by a decreasing slope over time (Fig. 2). Consequently, the uptake of [³H]oleic acid was inhibited by 23% after 1 min, 54% after 5 min, and 61% after 10 min of incubation.

To verify that filipin III also reduces uptake of other LCFAs, we investigated the uptake of [³H]stearic acid after filipin III preincubation and found a 44% reduction of radioactivity accumulation (55.2 ± 10.3 pmol mg protein^{-1} min^{-1} in the filipin III-treated cells compared with 98.6 ± 20.6 pmol mg protein^{-1} min^{-1} in the controls, $P < 0.01$) after 5 min incubation.

In summary, the inhibitory effect of filipin III on LCFA uptake was particularly strong in the later uptake phase
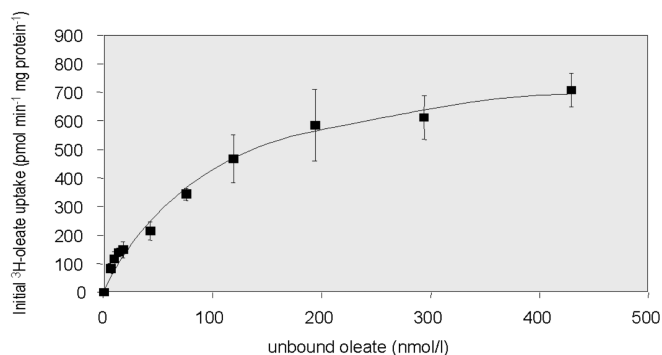
Fig. 1. Kinetic analysis of [³H]oleic acid uptake. Relationship between the initial rate of [³H]oleic acid uptake and unbound oleic acid concentrations. HepG2 cells were incubated with [³H]oleic acid bound to 173 μmol/l albumin in various molar ratios at 37°C in 2 ml of PBS for 20 s. The initial uptake exhibited saturable kinetics with $V_{max} = 854 \pm 46$ pmol mg protein^{-1} min^{-1} and $K_m = 100 \pm 14$ nmol/l. Values are means ± SD of five independent experiments.

Fig. 2. Filipin III effect on time course of [³H]oleic acid uptake. Incubation of 173 μmol/l [³H]oleic acid /BSA (1:1, mol/mol) with HepG2 at 37°C. Closed circle, control; open diamond, filipin III pretreatment (30 min). Values are means ± SD of five replicate experiments.

(>5 min) compared with the initial uptake phase (20 s). Thus, we used 5 min incubation experiments to further characterize the filipin III sensitive LCFA uptake mechanism by radioactive assays.
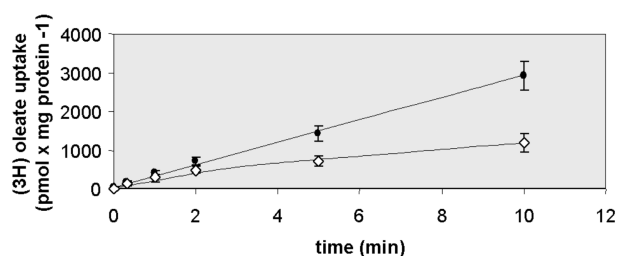
Metabolism of incorporated oleic acid

TLC analysis of intracellular lipids revealed that 67.6 ± 8.3% of the incorporated [³H]oleic acid was esterified to triglycerides and other complex lipids after 5 min. Another 15.7 ± 6.8% was recovered as acyl-CoA esters, while free oleic acid was virtually undetectable (values are means ± SD of three independent experiments). According to previous work of Stremmel et al. (7), after 5 min incubation period, the intracellular accumulation of radioactivity represents not only influx of LCFA, but is also the net effect of influx, efflux, and metabolization. It is theoretically conceivable that filipin III might exert its inhibitory effects on intracellular LCFA accumulation by interference with LCFA metabolism (e.g., by preventing esterification), which would allow for reflux of internalized LCFA out of the cells. However, TLC in the presence of filipin III revealed that, after 5 min of incubation, 72.4 ± 15.8% of the incorporated [³H]oleic acid were esterified and 16.2 ± 9.8% were recovered as acyl-CoA esters (values are means ± SD of three independent experiments), thus showing similar results as untreated HepG2 cells.

To further rule out interference of metabolization, we assessed the uptake of 12-NBD stearate, a fluorescent LCFA derivative that is neither metabolized nor excreted into bile (32, 33). TLC analysis showed that 12-NBD stearate was not metabolized even after 10 min of incubation with HepG2 cells (data not shown).

Effect of filipin III on 12-NBD stearate uptake in single HepG2 cells

The uptake of 12-NBD stearate follows the same kinetic features as the uptake of native LCFA (30). Elsing et al. (30) described a semi-quantitative, LSM-based method of visualizing and quantifying the uptake of 12-NBD stearate by hepatocytes on a subcellular level. We used this method to record the increase of fluorescence intensity in a previously defined cytosolic region of interest in a single cell as arbitrary units over time. A representative experiment using 23 μmol/l 12-NBD stearate and 150 μmol/l non-fluorescent stearic acid solubilized by 173 μmol albumin over a period of 10 min is illustrated in **Fig. 3**. The linear increase in cell fluorescence over the first 4 min represents cellular influx of 12-NBD stearate. However, beyond 4 min of incubation, the slope of the curve decreases indicating the presence of a self-quenching component. Following preincubation with filipin III, the uptake of 12-NBD stearate was inhibited by a similar degree as native [³H]oleic acid and [³H]stearic acid (Fig. 3).

Inhibitory effect of filipin III is reversible

We examined the reversibility of the effects of filipin III treatment on cells. HepG2 cell monolayers treated with filipin III for 30 min were washed and incubated for 30 min in standard cell culture media containing 20% FCS to replenish membrane cholesterol. Afterwards, HepG2 were processed through the usual [³H]oleic acid assay. **Figure 4** shows that this short reversal treatment resulted in restoration of normal [³H]oleic acid uptake levels in cells.

Effect of other vesicle inhibitors

We further tested the inhibitory effect of cholesterol depletion on LCFA uptake by pretreatment of HepG2 cells with cyclodextrin, another agent known to selectively inhibit caveolae by removing cholesterol from the plasma membrane (34, 35). Preincubation with cyclodextrin for 30 min yielded a 45% reduction of [³H]oleic acid accumulation (Fig. 4). Cholesterol depletion does not affect internalization of ligands via clathrin-coated pits (16) or in control experiments. Neither cyclodextrin nor filipin III affected the incorporation of ¹²⁵I-transferrin, which is taken up exclusively by clathrin-coated vesicles (36). Endocytosis via clathrin-coated pits is selectively reduced by depletion of intracellular potassium or incubation with hypertonic media (37). The uptake of [³H]oleic acid in HepG2 cells was not inhibited under these conditions (Fig. 4). In summary, the results suggest that caveolae but
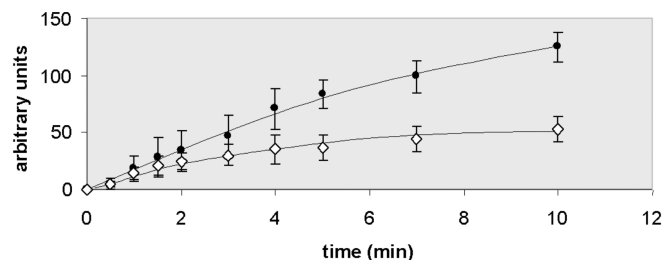
Fig. 3. Time course of 12-(N-methyl)-N-[(7-nitrobenz-2-oxa-1,3-diazol-4-yl)amino] (12-NBD) stearate uptake into single HepG2 cells. Time course of 12-NBD stearate uptake into a single HepG2 cell for 5 min. In this representative experiment 23 μmol/l 12-NBD stearate and 150 μmol/l non-fluorescent stearate in presence of 173 μmol/l BSA were incubated after (closed diamond) and without (open circle) preincubation with filipin III (5 μmol/l; 1 h at 37°C). Fluorescence intensity values, measured in arbitrary units, were recorded in an intracytoplasmatic region of interest. The intensity of the bulk solution did not significantly change during the observation period (data not shown). Values are means of 15–20 replicate experiments.

not clathrin-coated vesicles are operational in the uptake of [3H]oleic acid by HepG2 cells.

Antisense treatment to human caveolin-1 and clathrin

Caveolin-1 expression is an important prerequisite for the formation of caveolae (22, 23). In order to reduce levels of caveolin-1, we transfected HepG2 cells with antisense oligonucleotides to human caveolin-1. This resulted in a 50% reduction of cellular caveolin-1 protein content as assessed by Western blotting and densitometric scanning (**Fig. 5**). This translated to a 23% reduction of [3H]oleic acid uptake over 5 min (212 ± 13.4 pmol mg protein^{-1} min^{-1} and 273 ± 12.9 pmol mg protein^{-1} min^{-1} in cells treated with caveolin-1 antisense and controls, respectively ($P < 0.05$). Values are mean ± SD of five independent experiments. This inhibition is less than that afforded by filipin III and cyclodextrin. However,
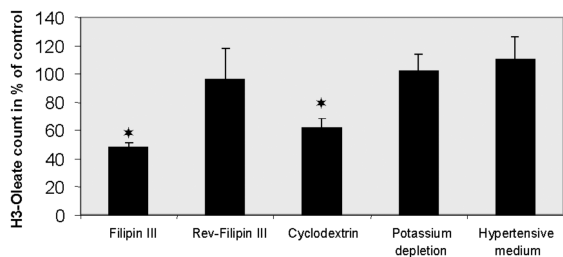

Fig. 4. Filipin III reversibility and effect of other inhibitors of vesicular mediated transport. HepG2 cells were pretreated with the inhibitors for 30 min. Incubation with 173 μmol/l albumin-bound [3H]oleic acid was carried out for 5 min. Rev-filipin III represents the accumulation of [3H]oleic acid achieved after attempting to reverse the filipin III effects using a 30 min incubation of the cells with standard medium plus 20% FCS as described in the text. Results are the percentage of uptake compared with controls (100%). One hundred percent are 1249 ± 105 pmol oleic acid/mg protein. The concentrations used were: filipin III, 5 μmol/l; cyclodextrin, 10 mmol/l. Values are means of five to seven replicate experiments. *Statistically significant differences by Student's t-test ($P < 0.01$).

since the reduction of caveolin-1 protein levels amounted to approximately 50%, a similar residual proportion of caveolae might still have been active in these cells, thus explaining the lower degree of oleic acid uptake inhibition effectuated by antisense treatment compared with the biochemical inhibitors. The equivalent sense strand served as control and neither changed the caveolin-1 protein content nor interfered with [3H]oleic acid uptake. Treatment with antisense to clathrin resulted in a 35% reduction of cellular clathrin content but did not result in any inhibition of [3H]oleic acid uptake (226 ± 14.2 pmol mg protein^{-1} min^{-1} in HepG2 cells treated with clathrin antisense versus 220 ± 25.2 pmol mg protein^{-1} min^{-1} in controls).

Microscopic visualization of endocytic vesicles

To further assess the intracellular trafficking and distribution of incorporated LCFA, we transfected α-caveolin-1/CFP chimeras into HepG2 cells. Caveolin-1/CFP was visible as distinct small single spots in the cytoplasm (**Fig. 6A**). When native caveolin-1 in non-transfected cells was detected by monoclonal antibody to caveolin-1 (Fig. 6B), it showed a very similar appearance compared with the α-caveolin-1/CFP construct. Indeed, immunofluorescence performed in cells transfected with α-caveolin-1/CFP before stained more vesicular structures (Fig. 6D) than α-caveolin-1/CFP alone (Fig. 6C), probably representing native caveolin-1 without CFP labeling. Transfection of CFP alone resulted in diffuse staining of the cytoplasm and the nuclei (Fig. 6E). To visualize involvement of caveolin-1 in intracellular trafficking of 12-NBD stearate, cells transfected with α-caveolin-1/CFP were incubated with a mixture of 12-NBD stearate (23 μmol/l) and non-fluorescent stearate (150 μmol/l) for 2 min in the presence of albumin at 37°C. Internalized 12-NBD dye (**Fig. 7A**) and CFP-labeled caveolae (Fig. 7B) showed a high degree of colocalization (Fig. 7C). 12-NBD stearate caused pronounced staining of intracellular membranes and some diffuse staining of the cytoplasm (Fig. 7A). Fluorescent fatty acids accumulated particularly in perinuclear and subplasmalemmal sections without significantly staining the plasma membrane.
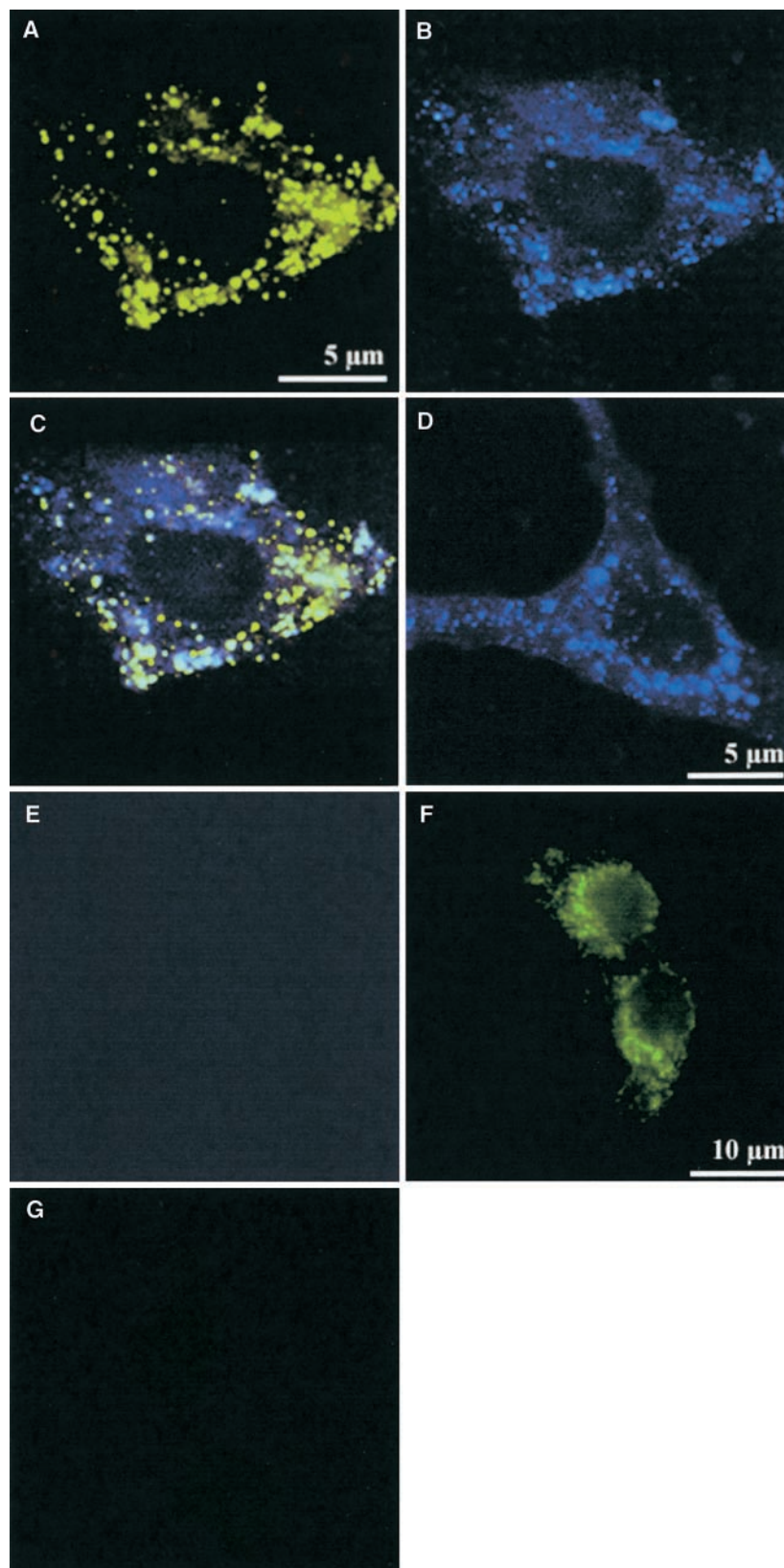
In control experiments, the specifity of the fluorescent filter systems was tested. Figure 7D, E show a caveolin-1 CFP transfected cell using the cyano (Fig. 7D) and the green fluorescent filter system (Fig. 7E). There is hardly any fluorescence observed using the green fluorescent filter system, thus proving the specifity of the signal. Figure 7F, G show a HepG2 cell that was incubated with 12-NBD
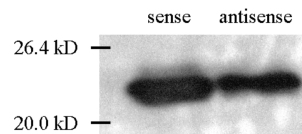
Fig. 5. Western blot detection of caveolin-1. Inhibition of caveolin-1 expression by antisense oligonucleotides to human caveolin-1. Controls include untreated cells and cells treated with the sense strand.
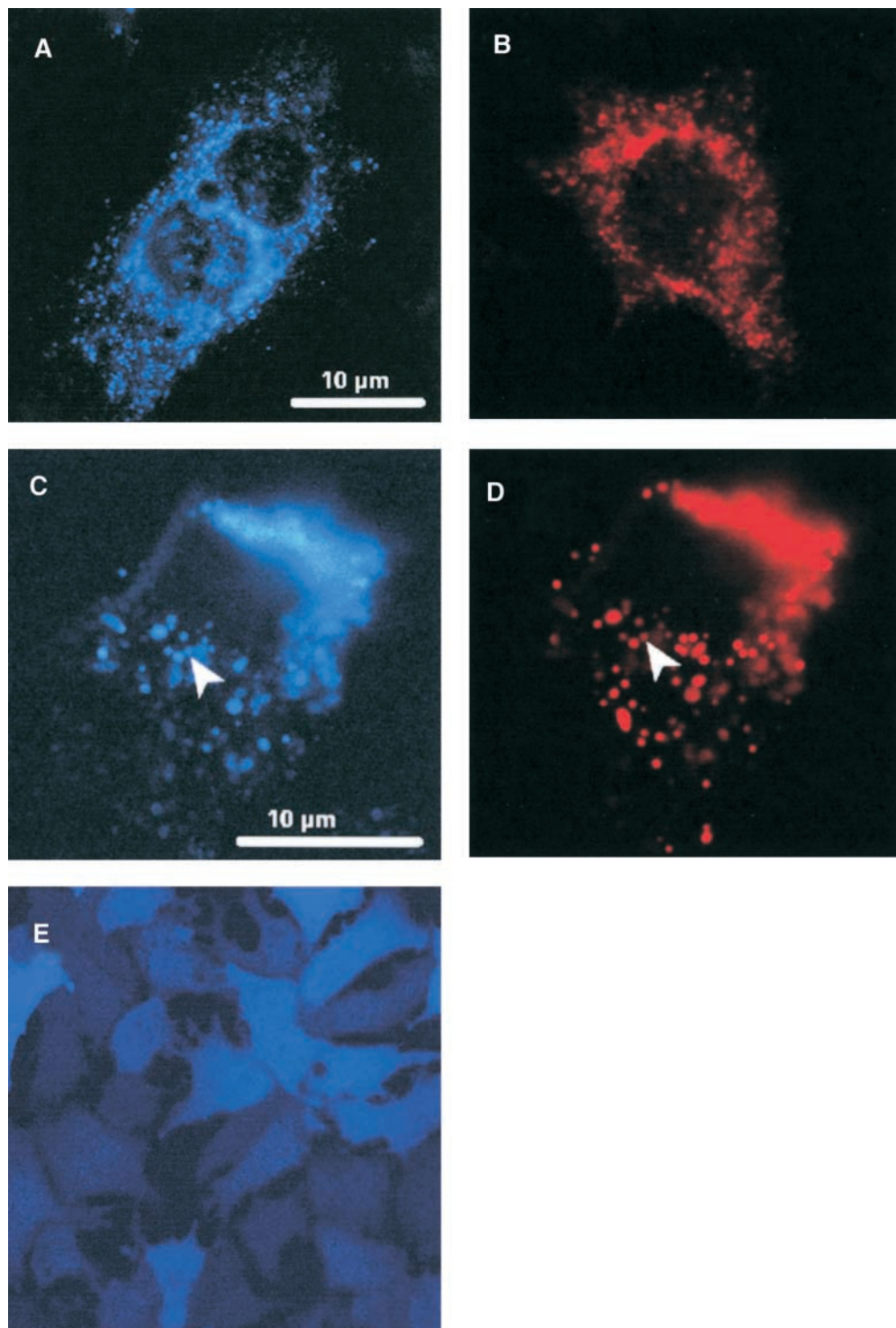
Fig. 6. Transfection of α-caveolin-1/CFP. Three days after transfection of α-caveolin-1/CFP into HepG2 cells, the CFP dye was visible as distinct small single spots in the cytoplasm (A) and had a similar appearance as native caveolin-1 detected cells by monoclonal antibody to caveolin-1 in non-transfected (B). Panels C and D show a representative HepG2 cell that was transfected with caveolin-1 construct and afterwards fixed, permeabilized, and labeled with murine monoclonal antibody against caveolin-1 followed by anti-mouse TRITC-conjugated secondary antibody. Note that CFP-labeled vesicles (C) were also detected by antibody against caveolin-1 (D). The arrowheads indicate identical vesicles showing significant colocalization. Immunofluorescence stained more vesicular structures than the CFP dye, probably representing native caveolae without inclusion of CFP. Transfection of CFP alone (E) resulted in diffuse staining of the cytoplasm and the nuclei (visualization by an inverted Olympus IX50 system).

Fig. 7. Colocalization of α-caveolin-1/CFP and 12-NBD stearate HepG2 cells transfected with α-caveolin-1/CFP were incubated with 12-NBD stearate for 2 min, fixed, and prepared for analysis by microscopy (inverted Olympus IX50 system). A: Shows the distribution of 12-NBD stearate and B shows α-caveolin-1/CFP. C: Merged image showing a high degree of overlap of CFP and 12-NBD dye labeling intracellular small vesicles. D and E: Show a caveolin-1 CFP transfected cell using the cyano (D) and the green fluorescent filter system (E). There is hardly any fluorescence observed using the green fluorescent filter system, thus proving the specifity of the signal. F and G: Show a HepG2 cell that was incubated with 12-NBD stearate for 2 min without prior caveolin-1 CFP transfection. While there is specific fluorescent staining using the green fluorescent filter system (F), there is no fluorescence detectable using the filters for CFP (G).

stearate for 2 min without prior caveolin-1 CFP transfection. While there is specific fluorescent staining using the green fluorescent filter system (Fig. 7F), there is no fluorescence detectable using the filters for CFP (Fig. 7G).
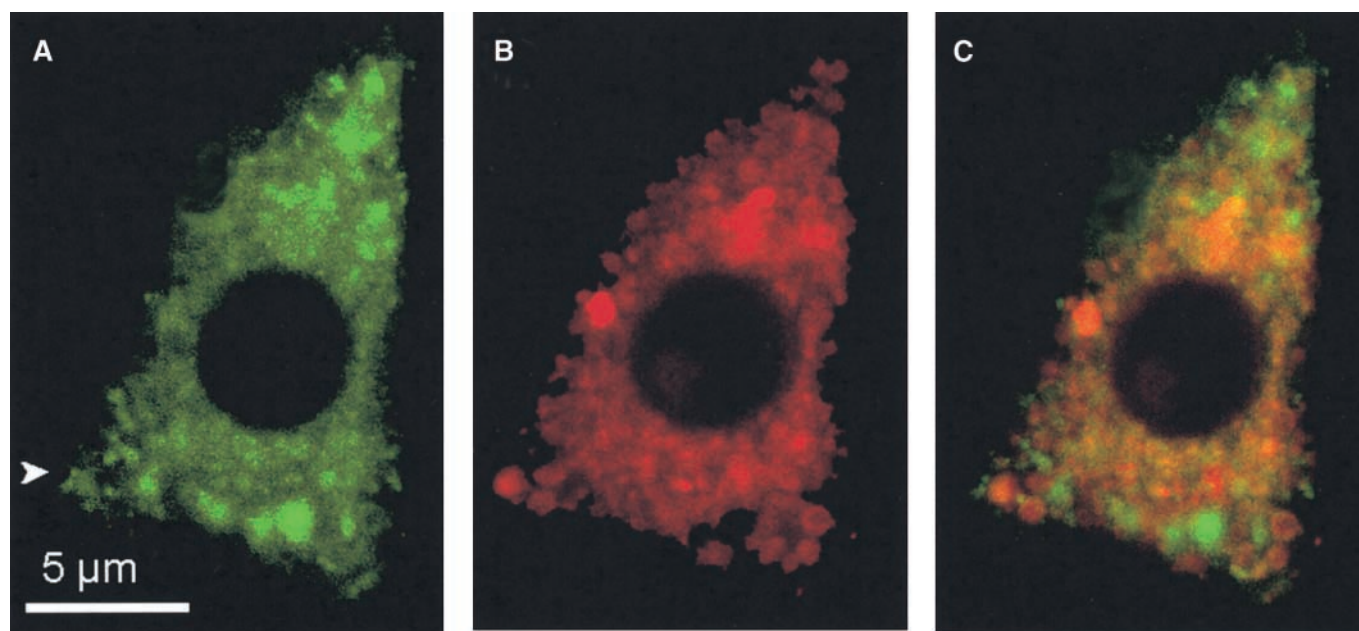
When the incubation with 12-NBD stearate was extended for 10 min, staining of larger organelles preferentially situated in the perinuclear region became evident (**Fig. 8A**). A portion of these structures was mitochondria, as assessed by the Mitochondrial Tracker fluorescent dye (Fig. 8B, C). However, since 12-NBD stearate is not metabolized, it is likely unable to enter mitochondria via the carnitine shuttle system. We assume that 12-NBD stearate is not internalized into mitochondria but is associated with the outer membrane of the organelle.

DISCUSSION

Endocytosis and vesicular transport are important functions for all cells, but they are particularly critical to hepatocytes, an epithelium that has a key role in metabolization and removes many different molecules from the blood and transfers them to bile. In this study, we present for the first time experimental data indicating contribution of caveolae vesicles to the uptake and intracellular trafficking of LCFA in HepG2 cells. Furthermore, we give evidence that HepG2 cells represent a valid and reliable model system to investigate LCFA uptake processes in hepatocytes. The experimental evidence is based both on biochemical and molecular caveolae inhibition studies as well as the microscopic visualization of LCFA binding to intracellular caveolae vesicles.

Cholesterol is the most important lipid component of caveolae required to maintain structural integrity of these membrane domains. Exposure to sterol-binding agents (e.g., filipin III and cyclodextrin) preferentially removes cholesterol from the plasma membrane, causing disassembly of caveolae and unclustering of receptors in caveolae (16, 31, 34, 38). Our inhibition experiments with filipin III and cyclodextrin suggest a caveolae-mediated LCFA uptake pathway in HepG2 cells that is operational predominantly in the later uptake phase. Oleic acid incorporation was also significantly reduced by inhibition of caveolae formation by antisense treatment to caveolin-1. The inhibition of the accumulation of the non-metabolizable fatty acid derivative 12-NBD stearate uptake by filipin III occurred to a comparable degree as the inhibition of native fatty acids. In addition, filipin III treatment did not affect LCFA metabolism in HepG2 cells. This indicates that *a*) filipin III-mediated inhibition of LCFA uptake is not due to interference of filipin III with LCFA metabolism, and *b*) 12-NBD stearate appears to be a suitable tool for microscopic LCFA uptake studies. After internalization by HepG2 cells, 12-NBD stearate significantly colocalized with α-caveolin-1/CFP, thus further consolidating the body of evidence supporting a role of caveolae for LCFA uptake and transport in hepatocytes. In contrast to caveolae, clathrin-coated vesicles do not appear to play a role in this process as neither antisense-treatment, nor depletion of intracellular potassium or hypertonicity afforded any inhibition of [³H]oleic acid uptake by HepG2 cells.

Fig. 8. Intracellular shift of 12-NBD stearate. A: Shows a HepG2 cell after 10 min incubation with 12-NBD stearate. Note that after prolonged incubation a significant portion of 12-NBD stearate associates with larger organelles preferentially situated in the perinuclear region. In double-labeling experiments with 12-NBD stearate (A) and Mitochondrial Tracker fluorescent dye (B) a main portion of these perinuclear structures can be identified as mitochondria. Merged images (C) show the locations of colocalization resulting in yellow fluorescence. Arrowhead indicates some remaining small vesicles next to the plasma membrane staining positive for 12-NBD stearate (visualization by an upright Zeiss LSM 310 system).

Which specific characteristics might render caveolae capable of LCFA uptake and transport? Caveolae harbor a specific set of membrane proteins that can bind and transport hydrophobic molecules like fatty acids and cholesterol. CD36/FAT, a protein that is involved in fatty acid uptake (11), and scavenger receptor class B type I, a receptor that mediates selective uptake of cholesterol esters, reside in caveolae (39, 40). Even more importantly, caveolin-1 can saturably bind fatty acids with high affinity (10, 41) and has a well-characterized function in the regulation of influx and efflux of cholesterol (14, 19, 38, 42). Apart from specific membrane proteins, the packing of cholesterol and sphingolipids into caveolae imposes a certain organization to the caveolar membrane that makes it biophysically distinct from the rest of the "fluid" phospholipid membrane (43, 44). It is not known if this peculiar structure influences flip-flop rates of LCFA. Gerber et al. [reported by Hui and Bernlohr (45)] proposed that LCFA diffuse into the open caveolae cavity. The pH of the cavity decreases when the cavity is closed, resulting in protonation of the LCFA followed by partitioning into the plasma membrane and passive diffusion across the bilayer. However, these are theoretical considerations and the molecular mechanism of caveolae-mediated uptake of LCFA awaits further investigation.

Our experimental data confirm previous studies showing that LCFA influx in HepG2 occurs rapidly. The initial uptake of LCFA (<1 min of incubation) is hardly inhibited by sterol-binding agents and most likely occurs via a protein carrier-facilitated mechanism, which is sensitive to phloretin, ouabain, antimycin A, and sodium azide. However, the filipin III sensitive vesicular pathway becomes more prominent with time and comprises 61% of the total uptake after 10 min. In the literature, there are only few and controversial data on the velocity and cargo capacity of caveolae mediated transport. A recent report by Pelkmans et al. (46) showed that simian virus 40 was internalized by caveolae and transported into intermediate organelles (termed caveosomes) with a half time of 60 min. It is not known yet if cargo size or a specific cargo binding protein can influence uptake velocity by inducing membrane-fission reactions that detach the caveolae from the plasma membrane as proposed by Pelkmans et al. (46).

Based on our data, we propose that at least two distinct pathways of LCFA uptake coexist in HepG2 cells: *a*) a rapid, filipin III insensitive mechanism operational predominantly in the first minute of uptake, and *b*) a slower, caveolae-mediated route that becomes predominant over time. The relative contribution of LCFA incorporation via caveolae compared with alternative uptake pathways cannot be derived from our data because filipin III might not inhibit all caveolae functions, as reported by Pol and coworkers (18) who identified an epidermal growth factor-activated and filipin III insensitive pathway of caveolae internalization in fibroblasts.

Apart from a substantial role of caveolae for LCFA uptake, our data further suggest the involvement of caveolae in intracellular LCFA trafficking. The insolubility of fatty acids in the aqueous environment of the cytosol requires specific intracellular trafficking mechanisms to deliver LCFA to subcellular organelles for metabolic needs. Our microscopic studies suggest that a significant amount of internalized 12-NBD stearate was localized to caveolae after 2 min of incubation, whereas after 10 min some of the fluorescent dye appeared to have moved on from caveolae toward other intracellular organelles, like mitochondria. Recently, Milliano and coworkers (47) investigated intracellular trafficking of 12-NBD stearate in primary hepatocytes by a laser photobleaching method and suggested that transport of 12-NBD stearate occurred predominantly by diffusion with no evidence for directed transport. They found excessive binding of 12-NBD stearate to endogenous membranes and proposed that cytosolic fatty acid binding protein (FABP) promotes trafficking by decreasing the amount of fatty acids bound to relatively immobile cytoplasmic membranes. However, their study did not assess the mobile fraction of endomembranes, which includes caveolae, and thus may have missed this alternative transport pathway described in our study.

In conclusion, our data support a role of caveolae for cellular uptake and intracellular trafficking of LCFA. The exact mechanism of LCFA translocation in the caveolar membrane awaits further investigation.■

REFERENCES

1. Distel, R. J., G. S. Robinson, and B. M. Spiegelman. 1992. Fatty acid regulation of gene expression. *J. Biol. Chem.* **267:** 5937–5941.
2. Amri, W-Z., G. Ailhaud, and P. A. Grimaldi. 1994. Fatty acids as signal transducing molecules: involvement in the differentiation of preadipose to adipose cells. *J. Lipid Res.* **35:** 930–937.
3. Noy, N., and D. Zakim. 1993. Physical chemical basis for the uptake of organic compounds by cells. *In*: Hepatic Transport and Bile Secretion. N. Tavoloni and P. D. Berk, editors. Raven Press, New York. 313–335
4. Hamilton, J. A., and F. Kamp. 1999. How are free fatty acids transported in membranes? Is it by proteins or by free diffusion through the lipids? *Diabetes.* **48:** 2255–2269.
5. Kleinfeld, A. M. 2000. Lipid phase fatty acid flip-flop, is it fast enough for cellular transport? *J. Membr. Biol.* **175:** 79–86.
6. Zakim, D. 2000. Thermodynamics of fatty acid transfer. *J. Membr. Biol.* **176:** 101–109.
7. Stremmel, W., and P. D. Berk. 1986. Hepatocellular influx of [¹⁴C] oleate reflects membrane transport rather than intracellular metabolism or binding. *Proc. Natl. Acad. Sci. USA*. **83:** 3086–3090.
8. Stremmel, W., G. Strohmeyer, F. Borchard, S. Kochwa, and P. D. Berk. 1985. Isolation and characterization of a fatty acid binding protein in rat liver plasma membranes. *Proc. Natl. Acad. Sci. USA.* **82:** 4–8.
9. Sorrentino, D., and P. D. Berk. 1993. Free fatty acids and the sinusoidal plasma membrane: Concepts, trends and controversies. *In:* Hepatic Transport and Bile Secretion. N. Tavoloni and P. D. Berk, editors. Raven Press, New York. 197–210
10. Trigatti, B. L., R. G. W. Anderson, and G. E. Gerber. 1999. Identifi-

cation of caveolin-1 as a fatty acid binding protein. *Biochem. Biophys. Res. Commun.* **255:** 34–39.

11. Abumrad, N. A., M. R. El-Maghrabi, E. Z. Amri, E. Lopez, and P. A. Grimaldi. 1993. Cloning of rat adipocyte membrane-protein implicated in binding or transport of long chain fatty acids that is induced during preadipocyte differentiation: homology with human CD 36. *J. Biol. Chem.* **268:** 17665–17668.

12. Lisanti, M. P., P. E. Scherer, Z-L. Tang, and M. Sargiacomo. 1994. Caveolae, caveolin and caveolin-rich membrane domains: a signalling hypothesis. *Trends Cell Biol.* **4:** 231–235.

13. Ros-Baró, A., C. Lopez-Iglesias, S. Peiro, D. Bellido, M. Palacin, A. Zorzano, and M. Camps. 2001. Lipid rafts are required for GLUT4 internalizationin adipose cells. *Proc. Natl. Acad. Sci. USA.* **98:** 12050–12055.

14. Fielding, P. E., and C. J. Fielding. 1996. Intracellular transport of low density lipoprotein derived free cholesterol begins at clathrin-coated pits and terminates at cell surface caveolae. *Biochemistry.* **35:** 14932–14938.

15. Anderson, R.G.W. 1993. Potocytosis of small molecules and ions by caveolae. *Trends Cell Biol.* **3:** 69–72.

16. Schnitzer, J. E., P. Oh, E. Pinney, and J. Allard. 1994. Filipin III-sensitive caveolae-mediated transport in endothelium: reduced transcytosis, scavenger endocytosis, and capillary permeability of select macromolecules. *J. Cell Biol.* **127:** 1217–1232.

17. Parton, R. G., B. Joggerst, and K. Simons. 1994. Regulated internalization of caveolae. *J. Cell Biol.* **127:** 1199–1215.

18. Pol, A., A. Lu, M. Pons, S. Peiro, and C. Enrich. 2000. Epidermal growth factor-mediated caveolin recruitment to early endosomes and MAPK activation. *J. Biol. Chem.* **275:** 30566–30572.

19. Conrad, P. A., E. J. Smart, Y. S. Ying, R. G. W. Anderson, and G. S. Bloom. 1995. Caveolin cycles between plasma membrane caveolae and the Golgi complex by microtubule-dependent and microtubule-independent steps. *J. Cell Biol.* **131:** 1421–1433.

20. Pol, A., M. Calvo, A. Lu, and C. Enrich. 1999. The "early-sorting" endocytic compartment of rat hepatocytes is involved in the intracellular pathway of caveolin-1 (VIP-21). *Hepatology.* **29:** 1848–1857.

21. Calvo, M., and C. Enrich. 2000. Biochemical analysis of a caveolae-enriched plasma membrane fraction from rat liver. *Electrophoresis.* **21:** 3386–3395.

22. Engelman, J. A., C. C. Wycoff, S. Yasuhara, K. S. Song, T. Okamoto, and M. P. Lisanti. 1997. Recombinant expression of caveolin-1 in oncogenically transformed cells abrogates anchorage-dependent growth. *J. Biol. Chem.* **272:** 16374.

23. Fra, A. M., E. Williamson, K. Simons, and R. G. Parton. 1995. De novo formation of caveolae in lymphocytes by expression of VIP21-caveolin. *Proc. Natl. Acad. Sci. USA.* **92:** 8655–8659.

24. Zhou, S. L., R. E. Gordon, M. Bradbury, D. Stump, C. L. Kiang, and P. D. Berk. 1998. Ethanol up-regulates fatty acid uptake and plasma membrane expression and export of mitochondrial aspartate aminotransferase in HepG2 cells. *Hepatology.* **27:** 1064–1074.

25. Gibbons, G. F., R. Khurana, A. Odwell, and M. C. Seelaender. 1994. Lipid balance in HepG2 cells: active synthesis and impaired mobilization. *J. Lipid Res.* **35:** 1801–1808.

26. Stremmel, W., G. Strohmeyer, and P. D. Berk. 1986. Hepatocellular uptake of oleate is energy dependent, sodium linked, and inhibited by an antibody to a hepatocyte plasma membrane fatty acid binding protein. *Proc. Natl. Acad. Sci. USA.* **83:** 3584–3588.

27. Wosilait, W. D., and P. A. Nagy. 1976. A method of computing drug distribution in plasma using stepwise association constants: clofibrate acid as an illustrative example. *Comput. Programs Biomed.* **6:** 142–148.

28. Spector, A. A., J. E. Fletcher, and J. D. Ashbrook. 1971. Analysis of long-chain free fatty acid binding to bovine serum albumin by determination of stepwise equilibrium constants. *Biochemistry.* **10:** 3229–3232.

29. Lamb, J. E., F. Ray, J. H. Ward, J. P. Kushner, and J. Kaplan. 1983. Internalization and subcellular localization of transferrin and transferrin receptors in HeLa cells. *J. Biol. Chem.* **258:** 8751–8758.

30. Elsing, C., U. Winn-Börner, and W. Stremmel. 1995. Confocal analysis of hepatocellular long-chain fatty acid uptake. *Am. J. Physiol.* **269:** 842–851.

31. Rothberg, K. G., J. E. Heuser, C. Donzell, Y. Ying, J. R. Glenney, and R. G. W. Anderson. 1992. Caveolin, a protein component of caveolae membrane coats. *Cell.* **68:** 673–682.

32. Fitz J.G., N.M. Bass, and R.A. Weisiger. 1991. Hepatic transport of a fluorescent stearate derivative: electrochemical driving forces in intact rat liver. *Am. J. Physiol.* **261:** G83–G91.

33. Bass, N. M. 1988. The cellular fatty acid binding proteins: aspects of structure, regulation, and function. *Int. Rev. Cytol.* **111:** 143–184.

34. Yancey, P. G., W. V. Rodrigueza, E. P. C. Kilsdonk, G. W. Stoudt, W. J. Johnson, M. C. Phillips, and G. H. Rothblat. 1996. Cellular cholesterol efflux mediated by cyclodextrins. Demonstration of kinetic pools and mechanism of efflux. *J. Biol. Chem.* **271:** 16026.

35. Parpal, S., M. Karlsson, H. Thorn, and P. Stralfors. 2001. Cholesterol depletion disrupts caveolae and insulin receptor signalling for metabolic control via insulin receptor substrate-1, but not for mitogen-activated protein kinase. *J. Biol. Chem.* **276:** 9670–9678.

36. Pearse, B., and M. S. Robinson. 1990. Clathrin, adaptors, and sorting. *Annu. Rev. Cell Biol.* **6:** 151–172.

37. Hansen, S. H., K. Sandvig, and B. Van Deurs. 1993. Clathrin and HA2 adaptors: effects of potassium depletion, hypertonic medium, and cytosol acidification. *J. Cell Biol.* **121:** 61–72.

38. Hailstones, D., L. S. Sleer, R. G. Parton, and K. K. Stanley. 1998. Regulation of caveolin and caveolae by cholesterol in MDCK cells. *J. Lipid Res.* **39:** 369–379.

39. Babitt, J., B. Trigatti, A. Rigotti, E. J. Smart, R. G. Anderson, S. Xu, and M. Krieger. 1997. Murine SR-BI, a high density lipoprotein receptor that mediates selective lipid uptake, is N-glycosylated and fatty acylated and colocalizes with plasma membrane caveolae. *J. Biol. Chem.* **272:** 13242–13249.

40. Malerød, L., L. K. Juvet, T. Gjøen, and T. Berg. 2002. The expression of scavenger receptor class B, type I (SR-BI) and caveolin-1 in parenchymal and nonparenchymal liver cells. *Cell Tissue Res.* **307:** 173–180.

41. Gerber, G. E., D. Mangroo, and B. L. Trigatti. 1993. Identification of high affinity membrane-bound fatty acid-binding proteins using a photoreactive fatty acid. *Mol. Cell. Biochem.* **123:** 39–44.

42. Smart, E. J., Y. S. Ying, P. A. Conrad, and R. G. W. Anderson. 1994. Caveolin moves from caveolae to the Golgi apparatus in response to cholesterol oxidation. *J. Cell Biol.* **127:** 1185–1197.

43. Smart, E. J., G. A. Graf, M. A. McNiven, W. C. Sessa, J. A. Engelman, P. E. Scherer, T. Okamoto, and M. P. Lisanti. 1999. Caveolins, liquid-ordered domains, and signal Transduction. *Mol. Cell. Biol.* **19:** 7289–7304.

44. Simons, K., and E. Ikonen. 1997. Functional rafts in cell membranes. *Nature.* **387:** 569–572.

45. Hui, Y., and D. A. Bernlohr. 1997. Fatty acid transporters in animal cells. *Front. Biosci.* **2:** 222–231.

46. Pelkmans, L., J. Kartenbeck, and A. Helenius. 2001. Caveolar endocytosis of simian virus 40 reveals a new two-step vesicular-transport pathway to the ER. *Nat. Cell Biol.* **3:** 473–484.

47. Milliano, M. T., and B. A. Luxon. 2001. The peroxisomal proliferator clofibrate enhances the hepatic cytoplasmic movement of fatty acids in rats. *Hepatology.* **33:** 413–418.